Syntheses, Crystal Structures and Properties of $[PPh_4]_2[SbFe_3H(CO)_{12}]$ and $[PPh_4]_2[AsFe_3H(CO)_{12}]$†

Peter Henderson,[a] Monica Rossignoli,[a] Robert C. Burns,*[,a] Marcia L. Scudder[b] and Donald C. Craig[b]

[a] *Department of Chemistry, The University of Newcastle, Callaghan 2308, New South Wales, Australia*
[b] *Department of Chemistry, The University of New South Wales, Kensington 2033, New South Wales, Australia*

Reaction of Sb_2O_3 or As_2O_3 with methanolic solutions of $Fe(CO)_5$–OH^- have resulted in the formation of the anionic species $[SbFe_3H(CO)_{12}]^{2-}$ or $[AsFe_3H(CO)_{12}]^{2-}$, which may be precipitated as their PPh_4^+ salts. The anions have also been obtained as the NEt_4^+, NMe_4^+ or $N(=PPh_3)_2^+$ salts. The PPh_4^+ salts of the anions are not isomorphous, with $[PPh_4]_2[SbFe_3H(CO)_{12}]$ crystallizing in the monoclinic space group $P2_1/c$, with $a = 11.165(5)$, $b = 49.223(9)$, $c = 10.903(5)$ Å, $\beta = 108.13(2)°$ and $Z = 4$, while $[PPh_4]_2[AsFe_3H(CO)_{12}]$ is triclinic, space group $P\bar{1}$, with $a = 12.088(5)$, $b = 13.257(5)$, $c = 19.389(8)$ Å, $\alpha = 80.43(3)$, $\beta = 83.55(3)$, $\gamma = 70.83(3)°$ and $Z = 2$. Each anion consists of a central antimony or arsenic atom surrounded by three $Fe(CO)_4$ groups in a trigonal-pyramidal arrangement, together with a hydrogen atom, although this was not crystallographically located and is inferred on the basis of charge considerations and, more importantly, ^1H NMR data. The Sb–Fe and As–Fe bond distances average 2.596(1) and 2.459(2) Å, respectively. The ^1H NMR spectra exhibit slightly broad singlets at δ −1.39 for $[SbFe_3H(CO)_{12}]^{2-}$ and δ 1.34 for $[AsFe_3H(CO)_{12}]^{2-}$, both with $w_{\frac{1}{2}}$ of *ca.* 6 Hz, which are indicative of hydrogen attached to antimony and arsenic. Attempts to synthesize the corresponding bismuth species were unsuccessful, which may be attributed to the poor Lewis basicity of the lone pair on bismuth and to the lack of stability displayed by a Bi–H bond. The reaction in this case generally results in the formation of $[BiFe_4(CO)_{16}]^{3-}$ and bismuth metal, likely involving the disproportionation of an anionic Bi^{III}–$Fe_m(CO)_n$ intermediate such as $[BiFe_3(CO)_{12}]^{3-}$, the deprotonated bismuth analogue of $[SbFe_3H(CO)_{12}]^{2-}$ and $[AsFe_3H(CO)_{12}]^{2-}$.

In recent years considerable attention has been directed towards the synthesis and properties of organotransition-metal species containing main group elements.[1] This has stemmed from the wide variety of structural features that these species exhibit, as well as their diverse chemical reactivities, and is particularly so for mixed organotransition-metal–main-group element cluster species with their potential impact in the area of catalysis.[2]

There have been several investigations into the synthesis and properties of iron carbonyl species in combination with the heavier elements of Group 15, primarily bismuth and antimony. This has led to the isolation and structural characterization of numerous open (*i.e.* non-cluster) species including the anions $[BiFe_4(CO)_{16}]^{3-}$ and $[SbFe_4(CO)_{16}]^{3-}$, where $[Fe(CO)_4]^{2-}$ formally acts as a ligand to a central Bi^V or Sb^V atom.[3–5] Further examples include the $[SbFe_3Cl(CO)_{12}]^{2-}$ and $[BiFe_3Cl(CO)_{12}]^{2-}$ ions, which also contain (formally) Sb^V and Bi^V.[5,6] Many other examples exist where an external $Fe(CO)_4$ group acts as a 'ligand' to a bismuth or antimony atom in a Bi–$Fe_m(CO)_n$ or Sb–$Fe_m(CO)_n$ cluster, such as occurs in the anions $[Bi_2Fe_4(CO)_{13}]^{2-}$, $[Bi_4Fe_4(CO)_{13}]^{2-}$, $[SbFe_4(CO)_{14}]^-$, $[Sb_2Fe_5(CO)_{17}]^{2-}$, $[SbFe_4H(CO)_{13}]^{2-}$ and $[SbFe_4H_2(CO)_{13}]^-$.[5,7–9] In several of these species some of the bismuth and antimony atoms can be formally regarded as being in the trivalent state. Moreover, in the case of S^{2-} or Se^{2-} 'ligands' evidence of, for example, Sb^{III} in species such as $SbSe_3$[3] can be found in the solid state in $Ba_4Sb_4Se_{11}$,[10] while anions such as $[SbS_4]^{3-}$ or $[AsSe_4]^{3-}$, which formally contain Sb^V or As^V are well known.[11] It was of interest, therefore, to examine the possibility of synthesizing the parent open M^{III} species (M = Bi, Sb or As) with $[Fe(CO)_4]^{2-}$ as the (formal) ligand, that is, the $[MFe_3(CO)_{12}]^{3-}$ species. Although these anions were not obtained, we report the syntheses, structures and characterization of the protonated forms of these species, *i.e.* $[MFe_3H(CO)_{12}]^{2-}$, where M is antimony or arsenic, together with an investigation into the analogous bismuth system.

Experimental

All operations and manipulations were performed under N_2 or in a vacuum so as to exclude oxygen, using Schlenk apparatus or an inert-atmosphere glove box (Vacuum Atmospheres HE-63P with a HE-493 Dri-Train). All reagents were used as received. Solvents were dried using standard methods and distilled under N_2 immediately before use, and were transferred with a gas-tight syringe.

Infrared spectra were recorded on a Bio-Rad FTS-7 spectrophotometer as KBr discs, Nujol mulls between NaCl plates or in solution using a 0.1 mm path length solution cell fitted with NaCl windows, while UV/VIS spectra were recorded on a Hitachi U-2000 spectrophotometer. All ^1H NMR spectra were recorded on a JEOL FX-90Q instrument operating at 89.60 MHz and were referenced to tetramethylsilane. X-Ray powder diffraction data were obtained using a Philips PW1700 Automated Powder Diffractometer System 1 employing Cu-Kα radiation. Microanalyses were performed by the Analytical Unit, Research School of Chemistry, at the Australian National University.

Synthesis of $[NEt_4]_2[SbFe_3H(CO)_{12}]$ *and* $[PPh_4]_2[SbFe_3H(CO)_{12}]$.—Under a flow of N_2, $Fe(CO)_5$ (2 cm^3, 15 mmol) was quickly added to a methanolic KOH (2.7 g) solution (20 cm^3) cooled in an ice–water bath. A slurry of Sb_2O_3 (0.725 g,

† *Supplementary data available:* see Instructions for Authors, *J. Chem. Soc., Dalton Trans.*, 1994, Issue 1, pp. xxiii–xxviii.

2.5 mmol) in methanol (30 cm^3) was slowly added to the stirred $Fe(CO)_5$–KOH solution, giving a deep red-brown solution. Dissolution of the Sb_2O_3 occurred quickly. After stirring for 1 h, a solution of NEt_4Br (2.3 g, 10.9 mmol) in methanol (30 cm^3) was added slowly to give a red-brown solid. The resulting material was isolated by filtration and dried in a vacuum (3.28 g, 74%). The compound may be purified by dissolution in methanol–acetonitrile, filtration, and subsequent cooling to −20 °C (Found: C, 37.7; H, 4.6; Fe, 18.2; N, 2.9; Sb, 13.3. Calc. for $C_{28}H_{41}Fe_3N_2O_{12}Sb$: C, 37.9; H, 4.7; N, 3.2; Sb, 13.7; Fe, 18.9%). The compound is soluble in acetonitrile, methanol, acetone and tetrahydrofuran (thf), but insoluble in toluene and light petroleum (b.p. 60–80 °C).

The PPh_4^+ salt was prepared in an identical way to that described above, using PPh_4Br in place of NEt_4Br, yielding 5.34 g (80%) of crude material. Crystals of this salt suitable for X-ray examination were grown by slow cooling of a saturated solution in MeOH–MeCN (70:20). IR (MeCN): ν_{CO} 2019w, 1988s, 1911s, 1901s, 1880m (sh) cm^{-1}. UV/VIS (MeCN–Uvasol): 433 (ε = 3200), 360 nm (5150 $dm^3\ mol^{-1}\ cm^{-1}$). ^1H NMR (CD_3CN): δ 7.7 (overlapping resonances, 40 H, Ph), −1.39 {br s, 1 H, $[SbFe_3H(CO)_{12}]^{2-}$}. Other salts have also been obtained using the same procedure, including compounds with NMe_4^+ or $N(=PPh_3)_2^+$ as the cations, by use of NMe_4Br and $N(=PPh_3)_2Cl$ in place of NEt_4Br.

Synthesis of $[PPh_4]_2[AsFe_3H(CO)_{12}]$.—A solution of $Fe(CO)_5$ in methanolic KOH was prepared as described above, and a slurry of As_2O_3 (0.504 g, 2.55 mmol) in methanol (30 cm^3) slowly added to the stirred solution. Dissolution of As_2O_3 occurred quickly to give a deep red solution. After stirring for 1 h, a solution of PPh_4Br (4.50 g, 10.7 mmol) in methanol (30 cm^3) was added giving a red-brown precipitate. The solid was filtered off and dried under vacuum (6.12 g, 94%). The crude material may be purified as described above. Crystals suitable for X-ray study were obtained by slow cooling of a saturated solution in MeOH–MeCN (70:15). IR (MeCN): ν_{CO} 2016w, 1988s, 1910 (sh), 1900s, 1881m (sh) cm^{-1}. UV/VIS (MeCN–Uvasol): 477 (ε = 2500), 373 nm (3500 $dm^3\ mol^{-1}\ cm^{-1}$). ^1H NMR (CD_3CN): δ 7.7 (overlapping resonances, 40 H, Ph), 1.34 {br s, 1 H, $[AsFe_3H(CO)_{12}]^{2-}$}.

Reaction of Bi_2O_3 *with Methanolic* $Fe(CO)_5$–KOH.—A solution of $Fe(CO)_5$ in methanolic KOH was obtained using the method described above. To this solution was added slowly a slurry of Bi_2O_3 (1.134 g, 2.43 mmol) in degassed water (or methanol) (50 cm^3), always maintaining the temperature of the mixture at *ca.* 0 °C using an ice–water bath. In the case of H_2O as solvent, the Bi_2O_3 dissolved fairly quickly and apparently completely to give a very dark brown solution. The reaction in methanol was much slower and always appeared incomplete, although giving the same dark brown solution. If the mixture at this stage was allowed to warm to room temperature, it slowly turned deep green with the concomitant formation of a metallic mirror on the inside walls of the reaction vessel. This was generally complete after 24 h. Filtration of the insoluble material followed by addition of a solution of NEt_4Br (5.25 g, 25.0 mmol) in methanol gave a deep green solid which was shown to be $[NEt_4]_3[BiFe_4(CO)_{16}]$ by infrared spectroscopy.[3] Examination of the insoluble material by X-ray powder diffraction indicated the presence of bismuth metal.

If, however, rather than allowing the brown solution to warm to room temperature, it was filtered at low temperature to remove undissolved Bi_2O_3, then a brown solid could be precipitated at *ca.* 0 °C by the addition of a solution of NEt_4Br (4.80 g, 22.8 mmol) in methanol. After filtration, washing with degassed H_2O (75 cm^3) and drying in a vacuum, 4.71 g of product were obtained. This solid appeared to be stable at room temperature in a N_2 atmosphere. The solid exhibited ν(CO) at 1972m, 1955 (sh), 1927s, 1870s, 1845s, and 1809s cm^{-1} (Nujol mull). Attempts to grow crystals of this material at low temperature (*ca.* −20 °C) from methanol or acetonitrile solution always resulted in the formation of deep green crystals of $[NEt_4]_3[BiFe_4(CO)_{16}]$ or, when acetone–light petroleum was used as solvent, the formation of $[NEt_4]_2[Bi_4Fe_4(CO)_{13}]$, as established by infrared spectroscopy.[8] This occurred even though on reconstitution in the appropriate solvent the resulting solution was always dark brown and was always handled below 0 °C to avoid thermal decomposition.

Deprotonation Reaction of $[SbFe_3H(CO)_{12}]^{2-}$ *using Potassium* tert-*Butoxide*.—To a solution of 0.500 g (0.38 mmol) of $[PPh_4]_2[SbFe_3H(CO)_{12}]$ in thf (50 cm^3) was added solid $KOBu^t$ (0.215 g, 1.92 mmol, a five-fold excess) in several portions. Reaction occurred immediately as evidenced by the change of the solution from orange to deep red. There was no evidence of solid formation. An infrared spectrum of this solution showed the presence of $[SbFe_4(CO)_{16}]^{3-}$ and some $[Sb_2Fe_5(CO)_{17}]^{2-}$, as well as other bands which have as yet not been identified.

Crystal Structure Determinations.—Crystal data. $[PPh_4]_2[SbFe_3H(CO)_{12}]$, M = 1305.2, monoclinic, space group $P2_1/c$, a = 11.165(5), b = 49.223(9), c = 10.903(5) Å, β = 108.13(2)°, U = 5694(4) $Å^3$, Z = 4, D_c = 1.52 g cm^{-3}, $F(000)$ = 1016, λ(Mo-Kα) = 0.7107 Å, μ(Mo-Kα) = 13.35 cm^{-1}, crystal size 0.03 × 0.07 × 0.26 mm.

$[PPh_4]_2[AsFe_3H(CO)_{12}]$, M = 1258.4, triclinic, space group $P\bar{1}$, a = 12.088(5), b = 13.257(5), c = 19.389(8) Å, α = 80.43(3), β = 83.55(3), γ = 70.83(3)°, U = 2888(2) $Å^3$, Z = 2, D_c = 1.45 g cm^{-3}, $F(000)$ = 998, λ(Mo-Kα) = 0.7107 Å, μ(Mo-Kα) = 14.23 cm^{-1}, crystal size 0.19 × 0.19 × 0.28 mm.

Data collection and processing. Reflection data were measured with an Enraf-Nonius CAD-4 diffractometer in θ–2θ scan mode for both crystals using graphite-monochromated Mo-Kα radiation. Both crystals showed some decomposition during data collection, probably arising from radiation damage, as they were coated for protection during data collection. The intensity of the standard reflections dropped to 0.80 and 0.70 for the antimony- and arsenic-containing compounds, respectively. Data were corrected for absorption by Gaussian integration using a 12 × 12 × 12 grid. For $[PPh_4]_2[SbFe_3H(CO)_{12}]$ a total of 6071 data were measured out to 2θ = 44° (a limit based on the decomposition of the crystal and the weakness of the high-angle data), giving a data set of 3733 reflections (minimum and maximum transmission factors of 0.87 and 0.96) with $I > 3\sigma(I)$ after averaging and accounting for the decay; R_{merge} = 0.020 for 289 pairs of equivalent 0*kl* reflections. For $[PPh_4]_2[AsFe_3H(CO)_{12}]$ a total of 10148 data were measured out to 2θ = 50°, giving a data set of 5965 reflections (minimum and maximum transmission factors of 0.78 and 0.82) with $I > 3\sigma(I)$ after averaging and accounting for the decay; R_{merge} = 0.009 for 342 pairs of equivalent 0*kl* reflections.

Structure determination. The structures were determined by Patterson and Fourier methods. Refinement used individual atom positional and anisotropic thermal parameters for the anions and phosphorus atoms, and rigid group positional and thermal parameters for the phenyl groups. The C–C and C–H bond distances were fixed at 1.395 and 1.0 Å, respectively, and the thermal parameters were refined as 12 parameter TL models with the centres of libration at the respective phosphorus atoms. Reflection weights used were $1/\sigma^2(F_o)$, with $\sigma(F_o)$ being derived from $\sigma(I_o) = [\sigma^2(I_o) + (0.04I_o)^2]^{\frac{1}{2}}$. Final residuals for $[PPh_4]_2[SbFe_3H(CO)_{12}]$ were R = 0.033 and R' = 0.039, while for $[PPh_4]_2[AsFe_3H(CO)_{12}]$ R = 0.051 and R' = 0.070, where the weighted residual is defined as $R' = (\Sigma w\Delta^2/\Sigma wF_o^2)^{\frac{1}{2}}$. Atomic scattering factors and anomalous dispersion parameters were from ref. 12. Structure solution used parts of the MULTAN 80 package,[13] and refinement used the comprehensive constrained least-squares refinement program RAELS 89.[14] The structural diagram was produced using ORTEP-II[15]

Table 1 Fractional atomic coordinates (non-hydrogen atoms) for $[PPh_4]_2[SbFe_3H(CO)_{12}]$ with estimated standard deviations (e.s.d.s) in parentheses

Atom	x	y	z	Atom	x	y	z
Sb	0.791 23(5)	0.122 45(1)	0.605 94(4)	C(42A)	0.224 1(7)	0.094 1(1)	0.385 7(6)
Fe(1)	0.894 6(1)	0.078 6(1)	0.553 0(1)	C(52A)	0.350 6(6)	0.086 4(1)	0.421 8(4)
Fe(2)	0.866 6(1)	0.137 5(1)	0.846 1(1)	C(62A)	0.394 0(4)	0.069 8(1)	0.340 4(4)
Fe(3)	0.759 8(1)	0.160 9(1)	0.436 0(1)	C(13A)	0.439 5(3)	0.060 6(1)	0.024 1(3)
C(1)	1.039 4(7)	0.092 9(2)	0.651 6(7)	C(23A)	0.510 3(5)	0.083 5(1)	0.078 9(4)
O(1)	1.135 3(6)	0.101 2(1)	0.714 0(6)	C(33A)	0.576 3(5)	0.097 8(1)	0.010 1(6)
C(2)	0.790 8(8)	0.061 4(2)	0.617 2(8)	C(43A)	0.571 7(5)	0.089 4(1)	−0.113 5(6)
O(2)	0.722 4(6)	0.049 0(1)	0.656 0(7)	C(53A)	0.500 9(6)	0.066 5(1)	−0.168 3(4)
C(3)	0.968 9(8)	0.049 7(2)	0.520 1(8)	C(63A)	0.434 9(5)	0.052 2(1)	−0.099 5(4)
O(3)	1.021 6(6)	0.031 2(1)	0.495 3(6)	C(14A)	0.249 4(3)	0.020 2(1)	0.013 9(3)
C(4)	0.836 6(7)	0.086 7(2)	0.387 7(7)	C(24A)	0.153 1(4)	0.033 6(1)	−0.079 7(4)
O(4)	0.802 7(6)	0.089 8(1)	0.276 9(5)	C(34A)	0.053 2(4)	0.018 8(1)	−0.161 2(4)
C(5)	0.903 4(8)	0.103 3(2)	0.889 5(7)	C(44A)	0.049 6(4)	−0.009 4(1)	−0.149 1(5)
O(5)	0.928 5(6)	0.081 3(1)	0.924 1(5)	C(54A)	0.146 0(5)	−0.022 8(1)	−0.055 5(6)
C(6)	0.910 5(8)	0.148 4(2)	1.006 5(7)	C(64A)	0.245 9(4)	−0.008 0(1)	0.026 0(4)
O(6)	0.935 4(7)	0.156 2(2)	1.110 9(5)	C(11B)	0.407 7(3)	0.234 2(1)	0.296 1(3)
C(7)	0.711 8(7)	0.149 7(1)	0.815 0(6)	C(21B)	0.409 3(4)	0.255 9(1)	0.214 3(4)
O(7)	0.610 6(5)	0.157 8(1)	0.798 8(5)	C(31B)	0.501 3(5)	0.276 0(1)	0.254 2(5)
C(8)	0.977 6(7)	0.157 3(1)	0.805 6(6)	C(41B)	0.591 7(5)	0.274 5(1)	0.375 8(6)
O(8)	1.052 3(5)	0.171 6(1)	0.782 8(5)	C(51B)	0.590 1(4)	0.252 7(1)	0.457 5(4)
C(9)	0.908 0(7)	0.149 8(2)	0.419 0(7)	C(61B)	0.498 1(4)	0.232 6(1)	0.417 6(3)
O(9)	0.997 8(5)	0.142 5(1)	0.401 0(5)	C(12B)	0.321 2(3)	0.183 8(1)	0.144 9(3)
C(10)	0.625 9(8)	0.141 9(1)	0.348 5(7)	C(22B)	0.255 9(4)	0.159 2(1)	0.128 8(5)
O(10)	0.537 0(5)	0.130 0(1)	0.292 3(5)	C(32B)	0.270 4(6)	0.140 2(1)	0.039 4(5)
C(11)	0.750 0(7)	0.183 7(1)	0.555 9(6)	C(42B)	0.350 1(6)	0.145 8(1)	−0.033 9(5)
O(11)	0.740 0(5)	0.199 5(1)	0.631 3(4)	C(52B)	0.415 4(6)	0.170 4(1)	−0.017 7(5)
C(12)	0.739 1(8)	0.186 6(2)	0.318 6(8)	C(62B)	0.401 0(4)	0.189 4(1)	0.071 6(4)
O(12)	0.723 4(7)	0.203 2(1)	0.240 6(5)	C(13B)	0.274 5(3)	0.192 1(1)	0.385 4(3)
P(A)	0.370 7(2)	0.040 4(1)	0.119 0(2)	C(23B)	0.181 1(4)	0.199 1(1)	0.440 1(4)
P(B)	0.287 7(2)	0.208 9(1)	0.246 6(2)	C(33B)	0.175 7(6)	0.186 0(1)	0.552 0(5)
C(11A)	0.490 8(3)	0.019 7(1)	0.224 3(3)	C(43B)	0.263 7(6)	0.166 0(1)	0.609 2(4)
C(21A)	0.458 1(4)	0.001 2(1)	0.305 4(4)	C(53B)	0.357 0(6)	0.158 9(1)	0.554 4(5)
C(31A)	0.551 4(6)	−0.014 4(1)	0.392 1(4)	C(63B)	0.362 4(4)	0.172 0(1)	0.442 6(4)
C(41A)	0.677 3(5)	−0.011 3(1)	0.397 7(4)	C(14B)	0.145 1(3)	0.225 7(1)	0.160 4(3)
C(51A)	0.710 0(3)	0.007 2(1)	0.316 5(5)	C(24B)	0.070 7(4)	0.215 5(1)	0.041 5(4)
C(61A)	0.616 7(3)	0.022 7(1)	0.229 8(4)	C(34B)	−0.040 0(4)	0.229 0(1)	−0.027 0(4)
C(12A)	0.310 8(3)	0.061 1(1)	0.222 9(3)	C(44B)	−0.076 4(4)	0.252 5(1)	0.023 2(6)
C(22A)	0.184 3(4)	0.068 9(1)	0.186 7(5)	C(54B)	−0.001 9(5)	0.262 7(1)	0.142 1(6)
C(32A)	0.141 0(5)	0.085 4(1)	0.268 1(6)	C(64B)	0.108 8(4)	0.249 3(1)	0.210 7(4)

running on a Macintosh IIcx, while an IBM 3090 computer was used for calculations. Atomic parameters and bond lengths and angles for both structures are given in Tables 1–4.

Additional material available from the Cambridge Crystallographic Data Centre comprises H-atom coordinates and thermal parameters.

Extended-Hückel Molecular Orbital Calculations.—Molecular orbital calculations were carried out using the extended-Hückel approach, as described by Hoffmann.[16,17] The basis set used for iron consisted of single Slater orbitals for both the 4s and 4p orbitals, while the 3d function was taken as a linear combination of two Slater-type functions. The Slater exponents (ζ) and valence-state ionization potentials (H_{ii}) for Fe, as well as those of Sb, As, C, O and H, were as reported in the literature.[16–20] Off-diagonal elements of the Hamiltonian, H_{ij}, were calculated using a modified Wolfsberg–Helmholtz formula[21] with $K = 1.75$. Calculations were carried out on both the isolated $[SbFe_3H(CO)_{12}]^{2-}$ and $[AsFe_3H(CO)_{12}]^{2-}$ ions.

Results and Discussion

Crystal Structures of $[PPh_4]_2[SbFe_3H(CO)_{12}]$ *and* $[PPh_4]_2[AsFe_3H(CO)_{12}]$.—The structures of both compounds consist of PPh_4^+ ions and either $[SbFe_3H(CO)_{12}]^{2-}$ or $[AsFe_3H(CO)_{12}]^{2-}$ ions. A view of the $[SbFe_3H(CO)_{12}]^{2-}$ ion is shown in Fig. 1. The $[AsFe_3H(CO)_{12}]^{2-}$ ion is almost identical. Both anions exhibit a trigonal-pyramidal arrangement of one Sb (or As) atom and three $Fe(CO)_4$ groups. For neither structure could the hydrogen in the anion be located and in each case is assumed to occupy the fourth site around the main group atom, which is supported by the ^1H NMR studies detailed below. The symmetry approximates to C_3 in each case, although this is not a crystallographic requirement. A hydrogen atom (formally H^+) completes the co-ordination of both antimony or arsenic, formally Sb^{III} or As^{III} and is therefore a source of electron density, resulting in Sb–H and As–H bonds.*

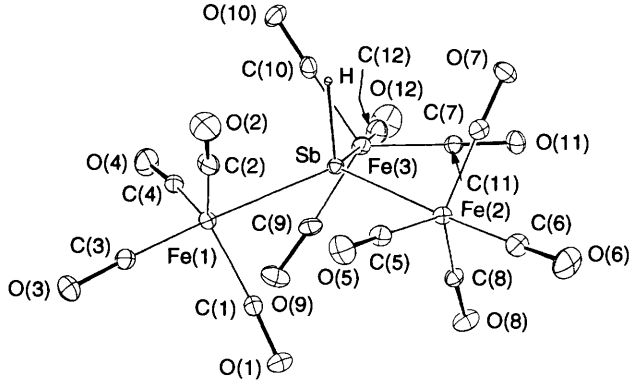

Fig. 1 View of the $[SbFe_3H(CO)_{12}]^{2-}$ ion. The hydrogen atom, although not crystallographically located, has been placed 1.707 Å from the antimony atom, which is the Sb–H distance found in SbH_3 (see text)

* Of course, the hydrogen could just as easily be regarded as H^-, making the formal oxidation state of both antimony and arsenic +5.

Table 2 Fractional atomic coordinates (non-hydrogen atoms) for $[PPh_4]_2[AsFe_3H(CO)_{12}]$ with e.s.d.s in parentheses

Atom	*x*	*y*	*z*	Atom	*x*	*y*	*z*
As	0.564 62(6)	0.102 52(5)	0.781 30(3)	C(42A)	0.609 6(6)	0.387 4(6)	0.276 7(3)
Fe(1)	0.618 47(9)	−0.027 92(7)	0.696 85(6)	C(52A)	0.699 2(6)	0.430 0(5)	0.249 1(3)
Fe(2)	0.679 83(8)	0.227 17(7)	0.767 67(5)	C(62A)	0.765 9(5)	0.396 2(4)	0.188 7(2)
Fe(3)	0.352 46(8)	0.179 99(8)	0.808 47(5)	C(13A)	0.744 2(3)	0.399 1(2)	0.007 8(2)
C(1)	0.641 6(8)	−0.122 7(6)	0.638 7(5)	C(23A)	0.663 1(4)	0.493 2(3)	0.028 3(2)
O(1)	0.653 3(7)	−0.184 8(5)	0.601 7(4)	C(33A)	0.608 5(4)	0.577 8(3)	−0.022 3(3)
C(2)	0.763 4(6)	−0.020 2(5)	0.684 0(4)	C(43A)	0.635 1(5)	0.568 4(4)	−0.093 4(3)
O(2)	0.858 1(5)	−0.021 2(5)	0.673 1(4)	C(53A)	0.716 3(5)	0.474 3(4)	−0.113 8(2)
C(3)	0.584 5(6)	−0.115 6(5)	0.771 1(4)	C(63A)	0.770 8(4)	0.389 7(3)	−0.063 2(2)
O(3)	0.566 6(5)	−0.172 9(4)	0.817 2(3)	C(14A)	0.964 3(3)	0.284 6(2)	0.075 0(2)
C(4)	0.511 5(7)	0.071 4(6)	0.641 3(4)	C(24A)	1.020 2(3)	0.335 8(3)	0.020 2(2)
O(4)	0.447 0(6)	0.130 6(5)	0.604 2(3)	C(34A)	1.139 8(4)	0.321 3(5)	0.021 0(3)
C(5)	0.772 8(7)	0.306 0(6)	0.753 3(4)	C(44A)	1.203 5(3)	0.255 7(5)	0.076 7(3)
O(5)	0.836 6(5)	0.356 7(5)	0.741 9(4)	C(54A)	1.147 5(3)	0.204 5(4)	0.131 5(3)
C(6)	0.578 4(7)	0.305 1(6)	0.826 4(4)	C(64A)	1.027 9(3)	0.219 0(3)	0.130 7(2)
O(6)	0.517 1(5)	0.360 1(5)	0.863 8(3)	C(11B)	0.957 8(3)	0.365 2(3)	0.388 5(2)
C(7)	0.793 4(7)	0.115 9(6)	0.804 2(4)	C(21B)	0.922 2(5)	0.474 5(3)	0.361 3(3)
O(7)	0.868 5(5)	0.045 2(5)	0.827 4(4)	C(31B)	0.976 1(6)	0.510 1(4)	0.298 8(3)
C(8)	0.644 5(6)	0.257 1(6)	0.679 1(4)	C(41B)	1.065 5(6)	0.436 6(6)	0.263 6(3)
O(8)	0.625 8(5)	0.278 2(5)	0.621 6(3)	C(51B)	1.101 1(5)	0.327 4(5)	0.290 9(3)
C(9)	0.204 6(7)	0.244 7(6)	0.831 5(4)	C(61B)	1.047 3(4)	0.291 7(4)	0.353 3(3)
O(9)	0.108 6(5)	0.286 1(5)	0.846 1(3)	C(12B)	0.991 6(3)	0.256 0(3)	0.530 6(2)
C(10)	0.325 5(6)	0.062 1(6)	0.792 0(4)	C(22B)	1.097 1(4)	0.279 6(4)	0.522 6(3)
O(10)	0.302 9(5)	−0.011 2(4)	0.782 2(3)	C(32B)	1.174 4(4)	0.243 3(6)	0.576 4(4)
C(11)	0.395 1(6)	0.177 8(6)	0.892 6(4)	C(42B)	1.146 3(6)	0.183 6(5)	0.638 2(3)
O(11)	0.420 3(5)	0.174 8(5)	0.949 1(3)	C(52B)	1.040 7(6)	0.160 1(5)	0.646 2(2)
C(12)	0.355 5(6)	0.278 4(5)	0.733 8(4)	C(62B)	0.963 4(5)	0.196 3(4)	0.592 4(2)
O(12)	0.351 9(5)	0.342 3(4)	0.685 9(3)	C(13B)	0.777 9(3)	0.428 1(2)	0.499 6(2)
P(A)	0.813 5(2)	0.292 5(1)	0.073 0(1)	C(23B)	0.794 1(4)	0.461 7(4)	0.561 2(2)
P(B)	0.886 3(2)	0.316 3(1)	0.467 1(1)	C(33B)	0.712 1(5)	0.553 0(4)	0.584 8(3)
C(11A)	0.805 1(3)	0.169 8(2)	0.053 0(2)	C(43B)	0.613 9(4)	0.610 7(3)	0.546 8(3)
C(21A)	0.710 8(4)	0.170 1(3)	0.017 4(3)	C(53B)	0.597 7(4)	0.577 0(4)	0.485 2(3)
C(31A)	0.702 7(5)	0.073 3(4)	0.002 7(3)	C(63B)	0.679 7(3)	0.485 7(3)	0.461 6(2)
C(41A)	0.788 9(5)	−0.023 9(3)	0.023 6(3)	C(14B)	0.819 0(4)	0.229 3(4)	0.439 4(3)
C(51A)	0.883 2(5)	−0.024 2(2)	0.059 2(3)	C(24B)	0.856 7(7)	0.184 4(6)	0.377 3(4)
C(61A)	0.891 3(4)	0.072 7(3)	0.073 9(3)	C(34B)	0.803 2(9)	0.115 4(7)	0.358 1(5)
C(12A)	0.743 0(3)	0.319 7(3)	0.155 8(2)	C(44B)	0.711 9(9)	0.091 2(7)	0.401 1(6)
C(22A)	0.653 4(4)	0.277 1(4)	0.183 4(3)	C(54B)	0.674 3(8)	0.136 1(8)	0.463 2(6)
C(32A)	0.586 8(5)	0.310 9(6)	0.243 9(3)	C(64B)	0.727 8(6)	0.205 1(6)	0.482 4(4)

Table 3 Bond lengths (Å) and angles (°) for $[PPh_4]_2[SbFe_3H(CO)_{12}]$ with e.s.d.s in parentheses

Sb–Fe(1)	2.597(1)	Sb–Fe(2)	2.597(1)	C(4)–O(4)	1.159(9)	C(5)–O(5)	1.152(9)
Sb–Fe(3)	2.594(1)	Fe(1)–C(1)	1.785(8)	C(6)–O(6)	1.151(9)	C(7)–O(7)	1.159(9)
Fe(1)–C(2)	1.746(8)	Fe(1)–C(3)	1.739(8)	C(8)–O(8)	1.176(9)	C(9)–O(9)	1.137(9)
Fe(1)–C(4)	1.760(7)	Fe(2)–C(5)	1.764(7)	C(10)–O(10)	1.151(9)	C(11)–O(11)	1.161(8)
Fe(2)–C(6)	1.747(8)	Fe(2)–C(7)	1.759(8)	C(12)–O(12)	1.154(10)	P(A)–C(11A)	1.788(3)
Fe(2)–C(8)	1.736(7)	Fe(3)–C(9)	1.807(8)	P(A)–C(12A)	1.799(4)	P(A)–C(13A)	1.774(4)
Fe(3)–C(10)	1.769(8)	Fe(3)–C(11)	1.752(7)	P(A)–C(14A)	1.780(4)	P(B)–C(11B)	1.784(4)
Fe(3)–C(12)	1.762(8)	C(1)–O(1)	1.151(9)	P(B)–C(12B)	1.776(4)	P(B)–C(13B)	1.772(4)
C(2)–O(2)	1.157(10)	C(3)–O(3)	1.162(10)	P(B)–C(14B)	1.780(4)		
Fe(1)–Sb–Fe(2)	115.8(1)	Fe(1)–Sb–Fe(3)	114.8(1)	Fe(1)–C(4)–O(4)	174.0(7)	Fe(2)–C(5)–O(5)	176.6(7)
Fe(2)–Sb–Fe(3)	116.1(1)	Sb–Fe(1)–C(1)	85.4(2)	Fe(2)–C(6)–O(6)	177.4(8)	Fe(2)–C(7)–O(7)	177.8(6)
Sb–Fe(1)–C(2)	85.2(2)	Sb–Fe(1)–C(3)	178.0(3)	Fe(2)–C(8)–O(8)	176.6(6)	Fe(3)–C(9)–O(9)	176.0(7)
C(1)–Fe(1)–C(2)	122.6(4)	C(1)–Fe(1)–C(3)	92.7(4)	Fe(3)–C(10)–O(10)	178.3(6)	Fe(3)–C(11)–O(11)	177.1(6)
C(2)–Fe(1)–C(3)	96.1(4)	Sb–Fe(2)–C(5)	88.4(2)	Fe(3)–C(12)–O(12)	178.7(8)	C(11A)–P(A)–C(12A)	105.7(2)
Sb–Fe(2)–C(6)	177.3(3)	Sb–Fe(2)–C(7)	85.0(2)	C(11A)–P(A)–C(13A)	108.7(2)	C(11A)–P(A)–C(14A)	111.3(2)
C(5)–Fe(2)–C(6)	93.1(4)	C(5)–Fe(2)–C(7)	120.6(4)	C(12A)–P(A)–C(13A)	111.3(2)	C(12A)–P(A)–C(14A)	111.3(2)
C(6)–Fe(2)–C(7)	92.4(4)	Sb–Fe(3)–C(9)	85.8(2)	C(13A)–P(A)–C(14A)	108.5(2)	C(11B)–P(B)–C(12B)	112.9(2)
Sb–Fe(3)–C(10)	84.5(2)	Sb–Fe(3)–C(11)	87.8(2)	C(11B)–P(B)–C(13B)	108.8(2)	C(11B)–P(B)–C(14B)	107.5(2)
C(9)–Fe(3)–C(10)	115.6(3)	C(9)–Fe(3)–C(11)	122.8(3)	C(12B)–P(B)–C(13B)	107.3(2)	C(12B)–P(B)–C(14B)	108.7(2)
C(10)–Fe(3)–C(11)	120.2(3)	Fe(1)–C(1)–O(1)	177.2(7)	C(13B)–P(B)–C(14B)	111.7(2)		
Fe(1)–C(2)–O(2)	176.6(7)	Fe(1)–C(3)–O(3)	176.8(7)				

For $[PPh_4]_2[SbFe_3H(CO)_{12}]$ all Sb–Fe distances are, within error, equivalent and average 2.596(1) Å, which is comparable to the average Sb–Fe distance in $[SbFe_4(CO)_{16}]^{3-}$ [2.666(3) Å][5] and the closely related $[SbFe_3Cl(CO)_{12}]^{2-}$ [2.565(4) Å],[5] both of which contain $Fe(CO)_4$ groups attached to antimony. In $[SbFe_4H(CO)_{13}]^{2-}$ and $[SbFe_4H_2(CO)_{13}]^{-}$, the Sb–Fe distances to the external $Fe(CO)_4$ groups are 2.521(2) and 2.5073(8) Å, respectively, while the Sb–Fe distances in both the tetrahedral $SbFe_3(CO)_9$ cluster units in these anions average 2.467(7) and 2.479(8) Å, respectively.[5] Likewise, in

Table 4 Bond lengths (Å) and angles (°) for $[PPh_4]_2[AsFe_3H(CO)_{12}]$ with e.s.d.s in parentheses

As–Fe(1)	2.461(1)	As–Fe(2)	2.454(1)	C(4)–O(4)	1.130(9)	C(5)–O(5)	1.161(10)
As–Fe(3)	2.461(1)	Fe(1)–C(1)	1.760(9)	C(6)–O(6)	1.142(9)	C(7)–O(7)	1.139(10)
Fe(1)–C(2)	1.775(7)	Fe(1)–C(3)	1.794(8)	C(8)–O(8)	1.134(9)	C(9)–O(9)	1.134(10)
Fe(1)–C(4)	1.814(7)	Fe(2)–C(5)	1.742(8)	C(10)–O(10)	1.142(9)	C(11)–O(11)	1.159(9)
Fe(2)–C(6)	1.765(7)	Fe(2)–C(7)	1.761(8)	C(12)–O(12)	1.143(8)	P(A)–C(11A)	1.770(3)
Fe(2)–C(8)	1.765(7)	Fe(3)–C(9)	1.752(8)	P(A)–C(12A)	1.766(4)	P(A)–C(13A)	1.779(4)
Fe(3)–C(10)	1.781(7)	Fe(3)–C(11)	1.759(7)	P(A)–C(14A)	1.795(4)	P(B)–C(11B)	1.798(4)
Fe(3)–C(12)	1.786(7)	C(1)–O(1)	1.144(11)	P(B)–C(12B)	1.770(4)	P(B)–C(13B)	1.778(4)
C(2)–O(2)	1.137(9)	C(3)–O(3)	1.123(10)	P(B)–C(14B)	1.790(5)		
Fe(1)–As–Fe(2)	115.5(1)	Fe(1)–As–Fe(3)	114.9(1)	Fe(1)–C(4)–O(4)	176.7(7)	Fe(2)–C(5)–O(5)	177.7(8)
Fe(2)–As–Fe(3)	116.3(1)	As–Fe(1)–C(1)	173.7(3)	Fe(2)–C(6)–O(6)	175.5(7)	Fe(2)–C(7)–O(7)	178.5(7)
As–Fe(1)–C(2)	91.3(2)	As–Fe(1)–C(3)	82.9(2)	Fe(2)–C(8)–O(8)	177.0(7)	Fe(3)–C(9)–O(9)	179.4(8)
C(1)–Fe(1)–C(2)	94.9(4)	C(1)–Fe(1)–C(3)	93.6(4)	Fe(3)–C(10)–O(10)	176.8(6)	Fe(3)–C(11)–O(11)	177.7(7)
C(2)–Fe(1)–C(3)	118.3(3)	As–Fe(2)–C(5)	174.1(3)	Fe(3)–C(12)–O(12)	176.8(7)	C(11A)–P(A)–C(12A)	111.0(2)
As–Fe(2)–C(6)	89.9(2)	As–Fe(2)–C(7)	85.9(2)	C(11A)–P(A)–C(13A)	108.9(2)	C(11A)–P(A)–C(14A)	109.9(2)
C(5)–Fe(2)–C(6)	96.0(4)	C(5)–Fe(2)–C(7)	90.6(4)	C(12A)–P(A)–C(13A)	109.1(2)	C(12A)–P(A)–C(14A)	108.1(2)
C(6)–Fe(2)–C(7)	117.2(4)	As–Fe(3)–C(9)	174.4(3)	C(13A)–P(A)–C(14A)	109.8(2)	C(11B)–P(B)–C(12B)	108.5(2)
As–Fe(3)–C(10)	91.9(2)	As–Fe(3)–C(11)	83.9(2)	C(11B)–P(B)–C(13B)	108.5(2)	C(11B)–P(B)–C(14B)	104.6(2)
C(9)–Fe(3)–C(10)	93.5(3)	C(9)–Fe(3)–C(11)	92.4(3)	C(12B)–P(B)–C(13B)	108.2(2)	C(12B)–P(B)–C(14B)	116.2(2)
C(10)–Fe(3)–C(11)	116.7(3)	Fe(1)–C(1)–O(1)	177.8(9)	C(13B)–P(B)–C(14B)	110.5(2)		
Fe(1)–C(2)–O(2)	175.1(7)	Fe(1)–C(3)–O(3)	177.8(6)				

$[Sb_2Fe_5(CO)_{17}]^{2-}$ and $[SbFe_4(CO)_{14}]^-$, the Sb–Fe distances to the external $Fe(CO)_4$ groups are 2.518(1) and 2.540(1) [there being two external $Fe(CO)_4$ groups in the former anion], and 2.481(3) Å, respectively, with the Sb–Fe distances in the $Sb_2Fe_3(CO)_9$ and $SbFe_3(CO)_{10}$ cluster units of these structures averaging 2.522 and 2.498 Å, respectively.[9] In both $[SbFe_4H(CO)_{13}]^{2-}$ and $[SbFe_4H_2(CO)_{13}]^-$ the Sb–Fe distance to the external $Fe(CO)_4$ group is significantly longer than the average Sb–Fe distance within the cluster unit, but in the last two examples all Sb–Fe distances are comparable. While it has been suggested that the longer Sb–Fe distances observed in $[SbFe_4(CO)_{16}]^{3-}$ (the longest observed Sb–Fe distances in these types of compounds) may be due in part to the steric requirements of four bulky $Fe(CO)_4$ groups surrounding antimony,[5] the trends for the other anions are not so evident. For $[SbFe_3H(CO)_{12}]^{2-}$ the steric demands are obviously less than for $[SbFe_4(CO)_{16}]^{3-}$ with hydrogen replacing an $Fe(CO)_4$ group, yet the Sb–Fe bond length is only a little shorter (by 0.070 Å). Surprisingly the average Sb–Fe bond length in $[SbFe_3H(CO)_{12}]^{2-}$ is longer than in $[SbFe_3Cl(CO)_{12}]^{2-}$ (by 0.031 Å), where steric effects would, at first sight, appear greater because of the bulkier chlorine atom. However, the respective Fe–Sb–Fe angles average 115.6 and 115.4°, thus indicating little steric difference between chlorine and hydrogen in this case, so that the difference in Sb–Fe bond lengths must be related to the difference in electronegativity between chlorine and hydrogen. In the examples containing cluster units, the main determining factor for Sb–Fe bond length presumably is related to the extent of back donation of electron density from Fe to CO in the $Fe(CO)_4$ units or $Fe_m(CO)_n$ cluster vertices, thereby influencing the ability of iron to share valence electrons with antimony. The presence of hydrogen, formally as H^+, would likely affect electron distribution in these species, along with the electron count of the actual cluster unit in the particular structure, but the investigation of such trends in these anions and their relationship to Sb–Fe distances based on the interpretation of CO stretching frequencies would be a complex study. Other Sb–Fe distances for comparison include those in the neutral species $[Sb_2Fe_6(CO)_{22}]$[22] which fall into two groups which average 2.497 and 2.557 Å, while in the binary phase $SbFe_2$ (a compressed marcasite structure) the average Sb–Fe distance is 2.590 Å.[23]

Very few examples are available for comparison with $[PPh_4]_2[AsFe_3H(CO)_{12}]$. The average As–Fe bond length in the anion is 2.459(2) Å, and comparisons include the (average) As–Fe bond length of 2.348(2) Å in the cluster species $[As_2Fe_3(CO)_9]$, 2.34(1) and 2.40(1) Å in $[As_2Fe_6(CO)_{22}]$ and 2.35 and 2.37 Å in $[AsFe_4Cl(CO)_{14}]$, although all three are neutral rather than anionic species.[24–26]

For all of the $Fe(CO)_4$ groups in both structures, the antimony or arsenic atom occupies the fifth co-ordination site giving a trigonal-bipyramidal geometry around iron in each case, and consequently an 18 valence-electron count. Thus no Fe–Fe bonds exist as evidenced by the (average) Fe···Fe distances of 4.393 and 4.160 Å for $[SbFe_3H(CO)_{12}]^{2-}$ and $[AsFe_3H(CO)_{12}]^{2-}$, respectively. There is no significant difference in either structure between the 'axial' and 'equatorial' Fe–C bond distances. The orientation of the $Fe(CO)_4$ groups with respect to each other is such that they minimize steric repulsions, with one CO group on each iron atom dovetailed between two CO groups on an adjacent iron atom. Thus, for example, CO(5) on Fe(2) is slotted between CO(1) and CO(2) on Fe(1) (see Fig. 1).

Unfortunately the hydrogen atoms in the structures could not be located which would have enabled a comparison with the values for Sb–H [1.707(3) Å] and As–H [1.519(2) Å] found for SbH_3 and AsH_3, as obtained from calculations based on precise microwave spectroscopic measurements.[27,28] In Fig. 1, the hydrogen has been included in the diagram at a distance of 1.707 Å from the antimony to complete the environment around this atom.

Synthesis and Properties of $[SbFe_3H(CO)_{12}]^{2-}$ *and* $[AsFe_3H(CO)_{12}]^{2-}$.—Both the $[SbFe_3H(CO)_{12}]^{2-}$ and $[AsFe_3H(CO)_{12}]^{2-}$ ions are easily synthesized by dissolution of Sb_2O_3 and As_2O_3, respectively, in methanolic $Fe(CO)_5$–KOH solutions using a 1:3 antimony (or arsenic) to iron mole ratio [equation (1)] (M = Sb or As). Both anions may be

$$M_2O_3 + 6\,[FeH(CO)_4]^- \longrightarrow 2\,[MH\{Fe(CO)_4\}_3]^{2-} + 2\,OH^- + H_2O \quad (1)$$

conveniently precipitated from solution as PPh_4^+, NEt_4^+, NMe_4^+ or $N(=PPh_3)_2^+$ salts. The presence of hydrogen as a component of these anions was positively established by ^1H NMR studies. The source of the hydrogen likely stems from abstraction of a proton from an $[FeH(CO)_4]^-$ ion during actual anion formation, as under the conditions of reaction $[Fe(CO)_4]^{2-}$ is completely protonated.[29] Less likely as a source of the hydrogen is $[HCO_3]^-$, which is produced in the prior formation of $[FeH(CO)_4]^-$ from $Fe(CO)_5$ on reaction with

OH^-. It should be noted that in previous investigations into the Sb–$Fe_m(CO)_n$ system, $SbCl_3$ (or $SbCl_5$) has been used as the source of antimony, or other chloride-containing species have been present such as $TlCl_3$.[5,6] This has resulted in the formation of $[SbFe_3Cl(CO)_{12}]^{2-}$ and, in the analogous bismuth system, $[BiFe_3Cl(CO)_{12}]^{2-}$. The use of Sb_2O_3 in place of $SbCl_3$ in this study therefore precludes the formation of $[SbFe_3Cl(CO)_{12}]^{2-}$, and likewise in the arsenic and bismuth systems, which leads to the observed products. Interestingly, the introduction of free chloride on addition of a tetraalkylammonium or related salt to precipitate the anion does not lead to substitution of the hydrogen and formation of, for example, $[SbFe_3Cl(CO)_{12}]^{2-}$ in the Sb–$Fe_m(CO)_n$ system.

The ^1H NMR studies of both compounds in CD_3CN gave slightly broad signals for the hydrogens attached to antimony or arsenic, with chemical shifts for $[SbFe_3H(CO)_{12}]^{2-}$ and $[AsFe_3H(CO)_{12}]^{2-}$ of δ −1.39 and +1.34, respectively, which are indicative of hydrogen bound to these elements. The values are significantly different to, for example, the hydrogen resonance at δ −8.74[30] in $[FeH(CO)_4]^-$ and to those found for a bridging hydrogen in $[NEt_4][SbFe_4H_2(CO)_{13}]$ (δ −22.63),[5] $[N(=PPh_3)_2][Fe_3H(CO)_{11}]$ (δ −14.53),[31] $[BiH_3Fe_3(CO)_9]$ (δ −24.1),[32] $[BiH_3Ru_3(CO)_9]$ (δ −17.73)[33] and $[BiH_3Os_3(CO)_9]$ (δ −19.9).[33] The values may be compared with those for SbH_3 and AsH_3, which occur at δ 1.38 and 1.50, respectively, (infinite dilution in CCl_4 at −20 °C).[34] Based on the electronegativities of antimony and arsenic compared to hydrogen, the relative chemical shifts of the protons in $[SbFe_3H(CO)_{12}]^{2-}$ and $[AsFe_3H(CO)_{12}]^{2-}$ are as expected, that is, greater shielding (a lower frequency) in the case of $[SbFe_3H(CO)_{12}]^{2-}$, which reflects the lower electronegativity of antimony. This trend is also shown by SbH_3 and AsH_3, although the difference in chemical shift is significantly smaller {$\Delta\delta$ = 0.12 in SbH_3 and AsH_3, *cf.* 2.73 in $[SbFe_3H(CO)_{12}]^{2-}$ and $[AsFe_3H(CO)_{12}]^{2-}$}. This is largely attributable to the relative number of hydrogen atoms bound to the single central antimony or arsenic atom. Thus the increase in electron density at hydrogen as a result of inductive effects in, for example, SbH_3 is diminished relative to the case in $[SbFe_3H(CO)_{12}]^{2-}$ because of the greater number of hydrogen atoms, leading to relatively less shielding and consequently to a higher frequency. The ^1H NMR resonances of $[SbFe_3H(CO)_{12}]^{2-}$ and $[AsFe_3H(CO)_{12}]^{2-}$ both exhibited a $w_{\frac{1}{2}}$ of 6 ± 1 Hz, with no evidence of fine structure. This is attributable to fast relaxation of the quadrupolar nuclei to which the hydrogens are attached so that the spin states of these nuclei cannot be distinguished (^{121}Sb, $I = \frac{5}{2}$, 57.25%, $Q = -0.53 \times 10^{-28}$ m^2; ^{123}Sb, $I = \frac{7}{2}$, 42.75%, $Q = -0.68 \times 10^{-28}$ m^2; ^{75}As, $I = \frac{3}{2}$, 100%, $Q = 0.3 \times 10^{-28}$ m^2).[35] Fast relaxation of the central quadrupolar nuclei in these two anions must certainly be associated with a lower than cubic symmetry (approximately C_3 in the solid state) leading to an electric-field gradient at the nucleus in each case.

Attempts to identify the Sb–H and As–H stretching frequencies for the two anions in their infrared spectra met with only partial success. Based on the ν(Sb–H) and ν(As–H) frequencies for SbH_3, AsH_3, and AsH_4^+, the Sb–H and As–H stretching frequencies for the two anions are expected to occur at about 2150–1800 cm^{-1}, just in the region where the extremely strong ν(CO) frequencies appear. Comparison of the infrared spectra (KBr discs) of the NEt_4^+, NMe_4^+, $N(=PPh_3)_2^+$ and PPh_4^+ salts of the two anions, in conjunction with their solution spectra, suggested that ν(As–H) in $[AsFe_3H(CO)_{12}]^{2-}$ occurred at 2038 cm^{-1}, but that the (lower frequency) ν(Sb–H) in $[SbFe_3H(CO)_{12}]^{2-}$ was masked by the much stronger ν(CO) vibrations of the $Fe(CO)_4$ groups.

The UV/VIS spectra of $[PPh_4]_2[SbFe_3H(CO)_{12}]$ and $[PPh_4]_2[AsFe_3H(CO)_{12}]$ exhibit strong bands at 433 and 477 nm, respectively. Both anions also exhibit a shoulder to higher energies, situated on another even stronger absorption below 300 nm in each case. The low energy absorption at 433 nm for the antimony compound can be compared to the absorption at 480 nm found for $[SbFe_4(CO)_{16}]^{3-}$, which was attributed to a ligand-to-metal charge-transfer transition. This was based on a comparison with the analogous $[BiFe_4(CO)_{16}]^{3-}$, which exhibits a band at 617 nm, and it was argued that the higher energy absorption for $[SbFe_4(CO)_{16}]^{3-}$ is consistent with the higher first ionization potential of antimony compared to bismuth and hence a ligand-to-metal charge-transfer transition.[5] If this is the case, then the trend to an analogous arsenic-containing compound would be to an even higher energy, in keeping with the correspondingly higher first ionization potential of arsenic. The trend observed for the related species synthesized in this study is, as evidenced by the values above, contrary to this expectation, with the absorption band of $[AsFe_3H(CO)_{12}]^{2-}$ occurring to *lower* energies than that of $[SbFe_3H(CO)_{12}]^{2-}$. This prompted us to perform extended-Hückel molecular orbital calculations on both anions, using idealised geometries (C_3) based on their crystallographically determined bond lengths and angles, with the hydrogen atoms located at the Sb–H and As–H bond distances found in SbH_3 and AsH_3, 1.707 and 1.519 Å respectively, in order to investigate the composition of the relevant orbitals.

The results of the calculations gave highest occupied molecular orbital (HOMO)–lowest unoccupied MO (LUMO) gaps of 3.12 eV (397 nm) and 3.06 eV (405 nm) for $[SbFe_3H(CO)_{12}]^{2-}$ and $[AsFe_3H(CO)_{12}]^{2-}$, respectively, in reasonable agreement with the experimental results (433 and 477 nm, respectively). The calculations indicate that the band for the arsenic compound should appear at lower energies, as is observed, although the calculated difference is minimal. However, given the limitations of the extended-Hückel approach, including the parametrization, the results are gratifying. More importantly, the calculations indicate that there are actually several levels in both anions which are close in energy to both the HOMO and LUMO, suggesting that the observed bands are likely composed of numerous overlapping transitions. Examination of the composition of all of these energy levels for each anion indicated that many have significant contributions from *both* metal and ligand orbitals. Furthermore, the HOMO for both anions has contributions from metal and ligand orbitals while the LUMO for both anions is ligand based. Thus the assignment of the lowest energy observed transition as a ligand-to-metal charge-transfer transition in these types of species may be a little simplistic.

Comparisons with the Analogous Bi–$Fe_m(CO)_n$ *System.*—Attempts to produce a stable bismuth anion analogous to $[SbFe_3H(CO)_{12}]^{2-}$ and $[AsFe_3H(CO)_{12}]^{2-}$ were unsuccessful. Reaction of Bi_2O_3 with a methanolic solution of $Fe(CO)_5$–OH^- at low temperature (*ca.* 0 °C) produced a very dark brown solution, from which a dark brown solid could be precipitated by addition of NEt_4Br. An infrared spectrum (Nujol mull) of this material indicated that it did not contain the analogous $[BiFe_3H(CO)_{12}]^{2-}$, but the ν(CO) profile was not indicative of any of the known anionic species in the Bi–$Fe_m(CO)_n$ system. Crystals grown from solutions of the brown solid in various solvents at low temperatures always contained $[BiFe_4(CO)_{16}]^{3-}$ as the anion, and in one case $[Bi_4Fe_4(CO)_{13}]^{2-}$. If the dark brown solution formed on dissolution of Bi_2O_3, added as an aqueous slurry to a methanolic solution of $Fe(CO)_5$–OH^-, was allowed to warm to room temperature, then bismuth metal formed in addition to a deep green solution of $[BiFe_4(CO)_{16}]^{3-}$. The disproportionation reaction of Bi^{III} into Bi^V and bismuth metal in this system can be written as in equation (2) where it is

$$5\,[BiFe_3(CO)_{12}]^{3-} \longrightarrow 3\,[BiFe_4(CO)_{16}]^{3-} + 2\,Bi + 3\,[Fe(CO)_4]^{2-} \quad (2)$$

proposed that the Bi^{III}–$Fe_m(CO)_n$ species that undergoes disproportionation is $[BiFe_3(CO)_{12}]^{3-}$, the deprotonated analogue of the antimony- and arsenic-containing species iso-

lated in this study. Indeed, the average ν(CO) stretching frequency of the dark brown anionic species obtained in the Bi–$Fe_m(CO)_n$ system is lower than that found for $[SbFe_3H(CO)_{12}]^{2-}$ and $[AsFe_3H(CO)_{12}]^{2-}$ {1896 *vs.* 1940 cm^{-1} in both $[SbFe_3H(CO)_{12}]^{2-}$ and $[AsFe_3H(CO)_{12}]^{2-}$, disregarding any possible degeneracies in the ν(CO) modes}, which is consistent with a more highly charged anion like $[BiFe_3(CO)_{12}]^{3-}$. It is also well established that bismuth(III) (with a lone pair of electrons) shows little Lewis basicity, so that protonation is less likely than in the corresponding antimony and arsenic systems. Moreover, it should be noted that comparison of the stabilities of the trivalent hydrides of arsenic, antimony and bismuth indicates that stability decreases markedly down this group, so that while AsH_3 and SbH_3 have been isolated (the latter decomposing slowly at room temperature), only trace amounts of BiH_3 have ever been isolated and the compound is only stable below −45 °C.[36] In contrast, all three trivalent chlorides are thermally stable at ambient temperatures and it is not surprising that the chlorobismuth species $[BiFe_3Cl(CO)_{12}]^{2-}$ has been reported to form, as has the chloroantimony species $[SbFe_3Cl(CO)_{12}]^{2-}$.[6]

The lack of stability of $[BiFe_3H(CO)_{12}]^{2-}$ suggests that deprotonation of $[SbFe_3H(CO)_{12}]^{2-}$ and $[AsFe_3H(CO)_{12}]^{2-}$, particularly the former, might result in analogous reactions to that given in equation (2) above. Indeed, treatment of $[SbFe_3H(CO)_{12}]^{2-}$ (as the PPh_4^+ salt) with excess potassium *tert*-butoxide in thf solution resulted in an immediate change in colour of the solution (orange to dark red), although no solid was observed to form. Infrared examination of the solution indicated the presence of $[SbFe_4(CO)_{16}]^{3-}$ and some $[Sb_2Fe_5(CO)_{17}]^{2-}$, as well as other unidentified peaks. Thus the deprotonation and subsequent disproportionation reaction of $[SbFe_3H(CO)_{12}]^{2-}$ is more complex than indicated by equation (2), although lending support to the interpretation suggested for the analogous bismuth system. A similar reaction also occurs in the arsenic system, presumably leading to new As–$Fe_m(CO)_n$ anionic species, and is currently under investigation.

Acknowledgements

The Australian Research Grants Scheme is acknowledged for financial support of this work, and Dr. D. Todd of the University X-Ray Centre is thanked for obtaining the X-ray powder diffraction data.

References

1 See, for example, K. H. Whitmire, *J. Coord. Chem.*, 1988, **17**, 95.
2 *The Chemistry of Metal Cluster Complexes*, eds. D. F. Shriver, H. D. Kaesz and R. D. Adams, VCH, New York, 1990.
3 K. H. Whitmire, C. B. Lagrone, M. R. Churchill, J. C. Fettinger and L. V. Biondi, *Inorg. Chem.*, 1984, **23**, 4227.
4 M. R. Churchill, J. C. Fettinger, K. H. Whitmire and C. B. Lagrone, *J. Organomet. Chem.*, 1986, **303**, 99.
5 S. Luo and K. Whitmire, *Inorg. Chem.*, 1989, **28**, 1424.
6 M. Ferrer, O. Rossell, M. Seco and P. Braunstein, *J. Organomet. Chem.*, 1989, **364**, C5.
7 K. H. Whitmire, M. Shieh, C. B. Lagrone, B. H. Robinson, M. R. Churchill, J. C. Fettinger and R. F. See, *Inorg. Chem.*, 1987, **26**, 2798.
8 K. H. Whitmire, M. R. Churchill and J. C. Fettinger, *J. Am. Chem. Soc.*, 1985, **107**, 1056.
9 K. H. Whitmire, J. S. Leigh, S. Luo, M. Shieh, M. D. Fabiano and A. L. Rheingold, *New J. Chem.*, 1988, **12**, 397.
10 G. Cordier, R. Cook and H. Schäfer, *Angew. Chem., Int. Ed. Engl.*, 1980, **19**, 324.
11 B. Krebs, *Angew. Chem., Int. Ed. Engl.*, 1983, **22**, 113, and refs. therein.
12 *International Tables for X-Ray Crystallography*, eds. J. A. Ibers and W. C. Hamilton, Kynoch Press, Birmingham, 1974, vol. 4.
13 P. Main, MULTAN 80, University of York, 1980.
14 A. D. Rae, RAELS 89, *A Comprehensive Constrained Least-Squares Refinement Program*, University of New South Wales, 1989.
15 C. K. Johnson, ORTEP-II, *A Thermal Ellipsoid Plotting Program*, Oak Ridge National Laboratories, TN, 1976.
16 R. Hoffmann and W. N. Lipscomb, *J. Chem. Phys.*, 1962, **36**, 2179, 3489.
17 R. Hoffmann, *J. Chem. Phys.*, 1962, **39**, 1397.
18 T. A. Albright, P. Hofmann and R. Hoffmann, *J. Am. Chem. Soc.*, 1977, **99**, 7546.
19 T. Hughbanks, R. Hoffmann, M.-H. Whangbo, K. R. Stewart, O. Eisenstein and E. Canadell, *J. Am. Chem. Soc.*, 1982, **104**, 3876.
20 D. J. Underwood, M. Nowak and R. Hoffmann, *J. Am. Chem. Soc.*, 1984, **106**, 2837.
21 J. H. Ammeter, H.-B. Bürgi, J. C. Thibeault and R. Hoffmann, *J. Am. Chem. Soc.*, 1978, **100**, 3686.
22 A. M. Arif, A. H. Cowley and M. Pakulski, *J. Chem. Soc., Chem. Commun.*, 1987, 622; A. L. Rheingold, S. J. Geib, M. Shieh and K. H. Whitmire, *Inorg. Chem.*, 1987, **26**, 463.
23 H. Holseth and A. Kjekshus, *Acta Chem. Scand.*, 1969, **23**, 3043.
24 L. T. J. Delbaere, L. J. Kruczynski and D. W. McBride, *J. Chem. Soc., Dalton Trans.*, 1973, 307.
25 L. J. Arnold, K. M. Mackay and B. K. Nicholson, *J. Organomet. Chem.*, 1990, **387**, 197.
26 G. Huttner, G. Mohr, B. Pritzlaff, J. von Seyerl and L. Zsolnai, *Chem. Ber.*, 1982, **115**, 2044.
27 A. W. Jache, G. S. Blevins and W. Gordy, *Phys. Rev.*, 1955, **97**, 680.
28 G. S. Blevins, A. W. Jache and W. Gordy, *Phys. Rev.*, 1955, **97**, 685.
29 H. W. Walker, C. T. Kresge, P. C. Ford and R. G. Pearson, *J. Am. Chem. Soc.*, 1979, **101**, 7428.
30 J. P. Collman, R. G. Finke, P. L. Matlock, R. Wahren, R. G. Komoto and J. I. Brauman, *J. Am. Chem. Soc.*, 1978, **100**, 1119.
31 H. A. Hodali and D. F. Shriver, *Inorg. Chem.*, 1979, **18**, 1236.
32 K. H. Whitmire, C. B. Lagrone and A. L. Rheingold, *Inorg. Chem.*, 1986, **25**, 2472.
33 H. G. Ang, C. M. Hay, B. F. G. Johnson, J. Lewis, P. R. Raithby and A. J. Whitton, *J. Organomet. Chem.*, 1987, **330**, C5.
34 E. V. A. Ebsworth and G. M. Sheldrick, *Trans. Faraday Soc.*, 1967, **63**, 1071.
35 R. K. Harris, *NMR and the Periodic Table*, eds. R. K. Harris and B. E. Mann, Academic Press, New York, 1978, ch. 1, p. 1.
36 J. D. Smith, *Comprehensive Inorganic Chemistry*, eds. J. C. Bailar, H. J. Emeléus, R. S. Nyholm and A. F. Trotman-Dickenson, Pergamon Press, Oxford, 1973, vol. 2, ch. 21, p. 547, and refs. therein.

Received 11*th November* 1993; *Paper* 3/06746G